This document is the accepted manuscript version of the following article:
Dauti, D., Tengattini, A., Pont, S. D., Toropovs, N., Briffaut, M., & Weber, B. (2020). Some observations on testing conditions of high-temperature experiments on concrete: an insight from neutron tomography. Transport in Porous Media, 132, 299-310. https://doi.org/10.1007/s11242-020-01392-2

Some observations on testing conditions of high-temperature experiments on concrete: an insight from neutron tomography

Dorjan Dauti · Alessandro Tengattini · Stefano Dal Pont · Nikolajs Toropovs · Matthieu Briffaut · Benedikt Weber

Abstract This communication explores the influence of boundary effects, embedded sensors and crack opening on high temperature experiments of concrete as revealed by *in-situ* neutron tomography. The hypotheses routinely taken about these experimental aspects in common practice are hereby reassessed in light of the insight given by non-invasive full-field measurements. Notably we directly assess the heat and moisture insulation techniques and reveal the influence of temperature and gas pressure monitoring on the testing conditions, opening new perspectives towards their improvement.

Dorjan Dauti
Université Grenoble Alpes, CNRS, Grenoble INP, 3SR, 38000 Grenoble, France
E-mail: dorjan.dauti@3sr-grenoble.fr

Alessandro Tengattini
Université Grenoble Alpes, CNRS, Grenoble INP, 3SR, 38000 Grenoble, France
Institut Laue-Langevin, 71 Avenue des Martyrs, 38000 Grenoble, France
E-mail: Alessandro.Tengattini@3sr-grenoble.fr

Stefano Dal Pont
Université Grenoble Alpes, CNRS, Grenoble INP, 3SR, 38000 Grenoble, France
E-mail: stefano.dalpont@3sr-grenoble.fr

Nikolajs Toropovs
Empa, Swiss Federal Laboratories for Materials Science and Technology, Überlandstrasse 129, 8600 Dübendorf, Switzerland
Riga Technical University, Institute of Materials and Structures, 1 Kalku Street, 1658, Riga, Latvia
E-mail: Nikolajs.Toropovs@empa.ch

Matthieu Briffaut
Université Grenoble Alpes, CNRS, Grenoble INP, 3SR, 38000 Grenoble, France
E-mail: matthieu.briffaut@3sr-grenoble.fr

Benedikt Weber
Empa, Swiss Federal Laboratories for Materials Science and Technology, Überlandstrasse 129, 8600 Dübendorf, Switzerland
E-mail: Benedikt.Weber@empa.ch

Keywords concrete · high temperature · neutron tomography · boundary effect · embedded elements

Article highlights

- Observation and quantification of the boundary effect, an important artifact in high temperature testing of concrete
- The formation of air bubbles due to thermocouple instrumentation
- The influence of a crack on the drying front inside concrete

1 Introduction

High-temperature behavior of concrete is an important issue for the structural safety of high-rise buildings, tunnels, nuclear power plants, etc. When these structures are exposed to fire, a phenomenon known as spalling may occur, which consists in the detachment of pieces of concrete from the heated surface. This phenomenon can lead to the premature failure of concrete structures. For better understanding the physics behind spalling, which is a rather complex phenomenon due to the coupled thermo-hydro-mechanical behaviour of heated concrete, many laboratory tests have been performed and are documented in the literature. Besides tests on full-scale concrete elements with typical size 3 m [1,2], tests on medium-scale specimens with a typical heated surface of 1 m^2 [3,4,5,6] and small-scale specimens (*e.g.* rectangular prisms or cylinders with edges or diameter/height less than 300 mm) [7,8,9,10,11,12,13,14] have been carried out. In most of these studies, the experimental procedure involves embedded elements such as thermocouples and pressure gauges inside concrete specimens to monitor the temperature and gas pressure field. In medium and small-size tests, which represent only a part of a structural element, some form of heat and moisture insulation is normally applied on the lateral sides of the samples aiming to achieve a uni-dimensional heat and moisture flow. For the moisture insulation, different approaches are routinely used. Self-adhesive aluminium foil was used in [13]. Felicetti et al. [15] tried two different sealing systems: (i) carbon fibers placed on a high-temperature silicon layer previously smeared on the concrete surface (ii) aluminium foil placed on the concrete surface after being both smeared with epoxy resin. The second system turned out to be a better insulator according to the mass loss results of a 120°C drying test in a ventilated oven. Also for the heat insulation, different options can be found in the literature. In [7,16] the lateral sides of the prismatic concrete samples were insulated by porous ceramics blocks. Van der Heijden et al. [10] insulated their sample with mineral wool. Toropovs et al., [13] used a 20 mm-thick glass foam layer in their neutron radiography tests of heated concrete. In [15,17] the authors covered their samples with ceramic fibre board.

In most of the aforementioned experiments, the validity of the boundary conditions is not directly measured. In this communication, observations from in-situ neutron tomography experiments are used to assess the underlying hypotheses. Some of the tests were presented in [18], where the focus was the analysis of the evolution of the moisture profiles, their relation to the temperature profiles, and the influence of the aggregate size on both. Here, we instead focus on some artefacts observed during the experiments, namely the influence of boundary conditions and measurement probes, which can help better appreciate the limit of the hypotheses used when interpreting many experimental results in literature. These observations rely heavily on the fact that 3D information is available from the tomography tests.

2 Neutron tomography experiments on heated concrete

In this section, a brief summary of the neutron tomography experiments is reported. More details can be found in [18]. Neutron tests show the evolution of moisture within the sample and enable thus much more detailed information than medium and large-scale test. However neutrons can penetrate concrete only through a few centimeters. This technique is thus only applicable to small samples. These tests were performed using cylindrical specimens with a diameter of 3 cm, which were cast using commercial plastic containers as mold, alongside with prismatic samples of $40 \times 40 \times 160\,\mathrm{mm}^3$ for mechanical properties. Mechanical properties were determined according to Swiss standard SIA 262-1 (similar to the European EN 12390-13 standard). In particular, compressive strength measured at 28 days on 6 samples (halves of initial 3 prisms used to determine flexural strength) resulted in 104.1 MPa. As the primary objective of the experimental study was to investigate the influence of the aggregate size, two different concrete mixes, with maximum aggregate size 8 mm and 4 mm (shown in Table 1), were used. The two mixtures, HPC 8 mm and HPC 4 mm, contained alluvial aggregates, like metamorphic rocks, with maximum diameter of 8 mm and 4 mm, respectively. The aggregate volume fraction for both mixtures was of 60% (of the *total* volume) The specimens were equipped with three thermocouples (type K) for temperature measurement at distances 3 mm, 10 mm, and 20 mm from the heated surface (see Figure 1). The two wires of the thermocouples enter the concrete radially from two sides and are welded together at the center. The location of the embedded thermocouples was imposed during concrete casting. In order to end up with a representative concrete heating surface at the top with a minimal amount of air bubbles, the samples were cast upside down with respect to the testing conditions. The thermocouples were thus located towards the bottom during casting. The samples were vibrated on a vibrating table until no more visible air bubbles appeared at the surface. Then they were sealed in plastic bags and stored in 97% relative humidity and 20°C. Neutron tomography measurements were performed 28 days after casting.

Similarly to [13, 15], the lateral surface of the sample was covered with self-adhesive aluminum tape, as shown in Figure 1, (virtually invisible to neutrons because of their very low interaction with aluminum) to prevent the vapor from escaping and to obtain a 1D movement of moisture within the heated sample. The aluminium tape used in the tests (3M High Temperature Aluminium Foil Tape 433) has a working temperature up to 316°C, which is higher than the temperature experienced by the sample during the test (~ 310°C).

The specimen was placed inside a heating cell (see Figure 2). During a test, the specimen was heated on the top face with a ceramic infrared radiator, which reached 500°C within 3 minutes and then was kept at constant temperature. The

Table 1 Concrete mixtures [kg/m^3]

	HPC 4 mm	HPC 8 mm
Cement CEM I 52.5 R	488	488
Silica fume	122	122
Aggregate 0−1 mm	632.8	400
Aggregate 1−4 mm	949.2	600
Aggregate 4−8 mm	0	582
Superplasticizer SIKA 20HE	8.54	8.54
Water	189.1	189.1
w/b total	0.31	0.31

Fig. 1 Specimen equipped with thermocouples and wrapped with adhesive aluminium tape (in testing orientation)

specimens were surrounded with rockwool, as shown in the drawing in Figure 2, in order to maximize the uniformity of one dimensional heating.

Neutron tomographies were performed at the NeXT(D50) beamline at the Institute Laue Langevin (ILL) in Grenoble, France. The principle of neutron tomography is analogous to that of x-ray computed tomography. However, in contrast to x-rays, which interact with electrons and whose attenuation thus depends on the atomic number of the atoms they interact with, neutrons interact with the nuclei. The hydrogen atoms of the water molecule highly attenuate neutrons, which makes it possible to detect the evolving moisture content in concrete. In addition, due to the presence of free and chemically bound water, the cement paste has higher neutron attenuation than the aggregates. Thus, the latter can be easily distinguished from the cement matrix. While the sample was being heated, neutron tomographies were performed for measuring in real time the moisture distribution in 3D (see Figure 3). During the heating test, 60 tomographies (3D scans) were taken. Each tomography, which comprised 500 projections, was acquired in only one minute. Such acquisition time was fast enough for following the rapid dehydration process in concrete.

3 Results and discussion

3.1 Boundary effects

One of the challenges when performing experiments on heated concrete is generating a uniform, “1D” heat and moisture flow by adopting the appropriate lateral heat and moisture insulation. Despite the applied insulation for heat and mois-

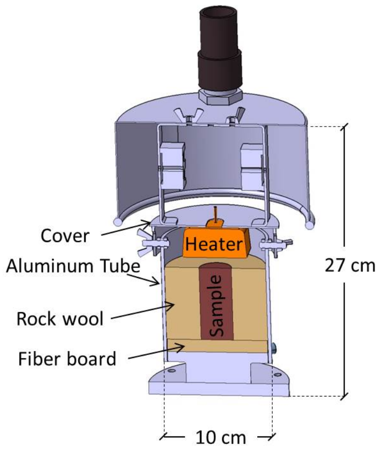

Fig. 2 Drawing of the heating cell

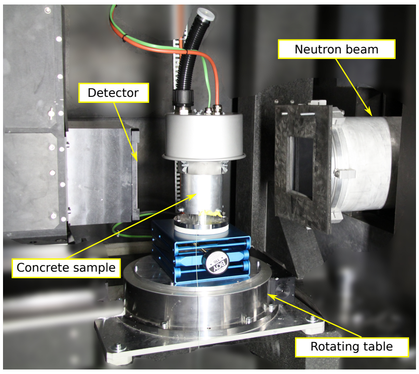

Fig. 3 Setup in the NeXT(D50) beamline at Institute Laue Langevin (ILL)

ture, drying at the boundary was observed in all the tested samples. An example of such a phenomenon is shown in the vertical cut of the 3D volume of sample HPC 8 mm given in Figure 4. Due to the difference in neutron attenuation between the hydrated and dehydrated cement paste, the drying front is evident in the image. It is clear that the front is not uniform and the precautions taken for obtaining a 1D drying front (rockwool and/or aluminium tape) are insufficient.

hypothetical explanation to this phenomenon could be the fact that because the specimens are cast, a 'wall effect' appears, meaning cement paste concentration near the mold. However, this hypothesis is not supported by the observations in [18], where the boundary effect is virtually identical regardless of the aggregate size (4 to 8 mm maximum diameter).

investigating further the effect of the self-adhesive aluminium foil, two concrete samples HPC 4 mm, with and without aluminum foil, were tested. As shown in Figure 4, the same boundary effect is observed in both samples. This shows that the influence of the aluminium tape is minimal.

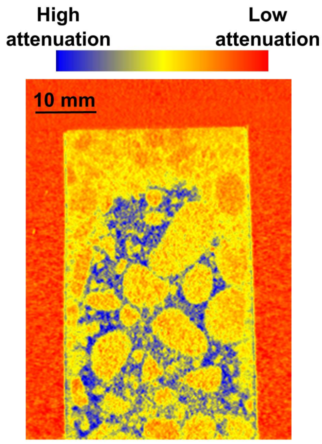

Fig. 4 Vertical cut of the 3D volume, captured at min 48 of heating, highlighting the additional lateral drying

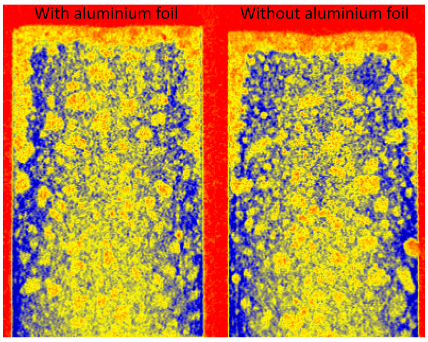

Fig. 5 Boundary effect in two samples, with and without aluminium foil

It is worth noting that, in the previous studies, such boundary effect was either assumed negligible in the analysis [7,15,19], or if it was detected, the 2D nature of the tests made it not quantifiable [13]. The 3D-measurements of moisture content by neutron tomography permits the observation and quantification of this boundary effect

The direct observation of the boundary effect opens new perspectives for investigating and eventually improving the current experimental practice on lateral insulation for achieving a uni-dimensional drying front. Realistic boundary conditions are not only important for reproducing as closely as possible the actual conditions of a concrete element submitted to fire, but it is also critical in quantifying important physical phenomena such as moisture accumulation. The aspects of the interaction of the boundary effect with the quantification of the moisture accumulation are discussed in the following.

In a situation where the drying front is not uniform, 3D measurements of moisture content by neutron tomography become even more relevant, and 1D or 2D measurements (*i.e*, neutron radiography, NMR, ground penetrating radar) have to be used with precaution. For instance, in neutron radiography, the recorded intensity is related to the neutron attenuation through the thickness of the sample parallel to the neutron beam. A radiography is a projection resulting from the integration of the signal attenuation in the direction of the beam. The 1D profile is then evaluated by averaging the projection perpendicular to the beam (see [13]). The boundary effects perpendicular to the neutron beam can be eliminated by considering only an interior region of the radiography. The boundary effect in the beam direction, however, is inherently inextricable in the radiography. This can give misleading results.

As an example, the averaging process as obtained from radiography is compared to the averaging obtained from tomography in Figure 6(a). The two processes correspond to two different regions:

– The first region is a disc which excludes the boundaries and represents a region where the front is uniform.

– The second region is a slice in which we exclude the boundaries only in one direction. Such a region would be representative of the one-dimensional moisture profiles usually obtained from neutron radiography experiments.

The thickness of the disk is of 20 pixels i.e. 4 millimeters. The purpose of a “thick” disk is merely to reduce statistical noise induced by the high speed of the acquisitions. As such, thinner disk are more noisy but also more spatially detailed.

In Figure 6(b), the evolution of the average gray value with time for the two regions is compared. Note that what is perceived as gray value in the images is actually directly related to the water content: a high gray value means a high water content. The ’gray’ images in Figure 4 and 5 are transformed to color composite images, where blue color means high gray value (high water content). In Figure 6(b) the results of the average gray value have been normalized to the initial gray value.

A clear difference between the two can be observed. In the disc, an increase in the gray value is seen, while the gray value in the slice doesn’t exhibit such an increase due to the boundary effect, which still exists in one direction. An increase in the core is in fact hidden by a decrease near the boundary. This simple example highlights another aspect of the importance of 3D measurements.

While the example above demonstrates how the boundary effect can cause an underestimation of the moisture accumulation, it was shown in a previous study [18] that the boundary effect can also cause an overestimation of the moisture accumulation when a neutron imaging artefact such as beam hardening takes place. A simplified model for estimating the influence of beam hardening showed that this artefact, together with lateral drying, makes the moisture accumulation appear more pronounced than it actually is.

3.2 Thermocouple-induced air bubbles

Embedded elements (*e.g.* thermocouples, pressure sensors) are routinely employed in experiments for measuring parameters such as temperature or pressure in heated

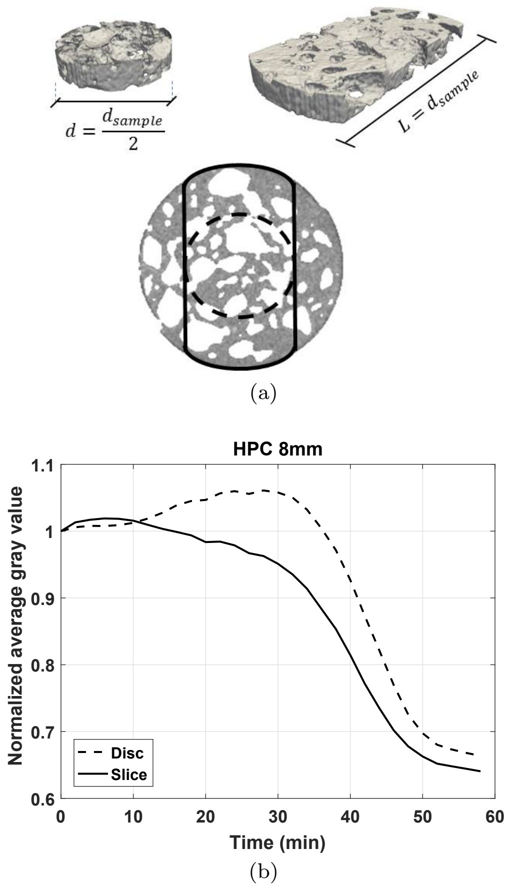

Fig. 6 Moisture profiles for two regions: a disc (representing the analysis performed in the current study using the neutron tomography results) and a slice (representing the analysis usually performed using neutron radiography results), both represented schematically in (a). The results, given in (b) show how the 1D-profiles obtained from neutron radiography (solid line) can be misleading due to the boundary effect which is not visible in the direction of the beam

concrete, which are useful for understanding the behaviour of concrete at high temperature. Nevertheless, the presence of such elements inside concrete might perturb the sample and affect the measurement. For instance, in [20], it is postulated that a cavity, possibly formed around the head of the pressure gauge, has an influence on the pressure measurement. Similarly, in [21], it is claimed that a cavity might be formed around a thermocouple, resulting in a plateau in the temperature development around 100°C, which is an experimental anomaly often observed because of the fact that the cavity becomes water-filled and the thermocouple measures the temperature inside the cavity.

Unlike in the aforementioned works, where possible defects are hypothesized, in the reported neutron experiments this alteration of the samples induced by the presence of thermocouples was observed directly, for the first time. Figure 7 shows

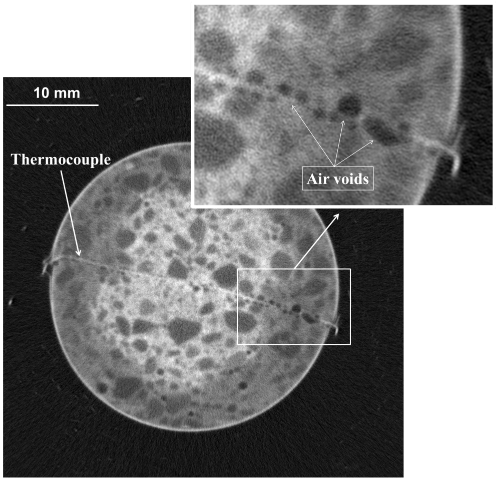

Fig. 7 Air voids around a thermocouple in a high resolution image

a horizontal slice at the position of the thermocouple located 20 mm from the heated surface of a sample with HPC 4 mm concrete mix. Air voids are observed around the thermocouple wire which has a diameter of only 0.25 mm. It appears that these air bubbles rose during casting when vibrating and were trapped in the proximity of the wires.

This is an important observation for the experimental community on heated concrete, which indicates that even very thin embedded elements such as a thermocouple can be intrusive and can affect locally the material properties and eventually the measurement that is being performed. Such an artefact can become even more substantial when considering other embedded measurement elements such as pressure sensors, the size of which can range from 2 mm to 12 mm [22]. Similarly to what is observed for the thermocouples in Figure 7, air voids around a pressure sensor could build an escape channel for vapor and potentially affect the pressure measurements, which have been extensively used in literature for validating numerical models. While several hypotheses have been postulated in literature on the disturbance caused by an embedded element [21, 22, 23], neutron imaging represents an effective method for having a closer look to such perturbations in order to improve the measurement procedures.

Using neutron imaging, it is also possible to accurately determine the exact position of a thermocouple. This useful information becomes particularly relevant when considering the validation of numerical models, as even a small change in the position causes a significant difference in the temperature results as shown in [24].

3.3 Influence of a crack on the drying front

The concrete samples employed in heating tests may contain pre-existing cracks due to a number of reasons including shrinkage, disturbance by the embedded

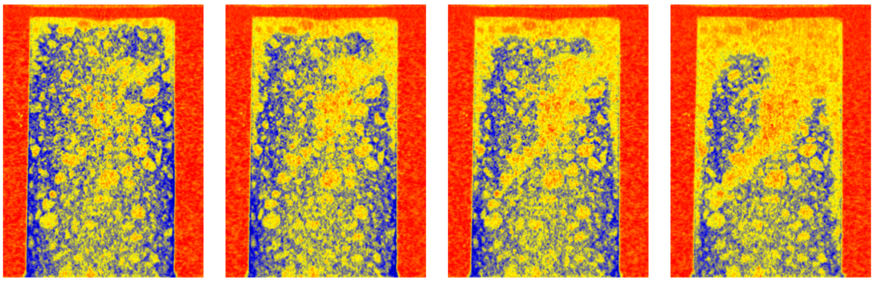

Fig. 8 Vertical cut at (a) 20 min (b) 26 min (c) 30 min (d) 42 min

elements, demolding etc. In addition, cracks may form during heating (high temperature gradients, thermal incompatibility aggregate-cement paste etc). These cracks often go unnoticed since they are too small to be detected by the naked eye or are located inside the sample. In this section, the detection and the influence that a crack can have on the drying front is discussed.

A heating test in which a crack has been observed to influence the drying front is presented in the following. Note that the experimental procedure followed for this test is the same as the one described in Section 2. The sample (HPC 4 mm) was equipped with thermocouples and no crack was observable when looking at the sample with naked eye before the test. Vertical slices of the tomographies, obtained at different times, are shown in Figure 8. A diagonal crack, initiated at the position of the thermocouple, possibly due to the voids surrounding it, created a diagonal drying path alongside it. The reason may be related to the physical process of dehydration occurring predominantly around a crack, where vapor can escape and the pore pressure is low.

4 Conclusion

Neutron tomography experiments on concrete have revealed important information related to the commonplace experimental procedures employed in the study of the behavior of concrete at high temperature with respect to spalling.

It has been observed that the heat and moisture insulation techniques that have been adopted in this study, as well as in other studies in literature, are not sufficient, as all the tested samples experience some degree of lateral drying. This yields a non-uniform drying front, which not only affects the representativity of the sample with respect to a concrete element subjected to fire, but is also critical in quantifying important physical phenomena such as moisture accumulation.

Tomography images have shown that air voids can form around thermocouples resulting in a perturbation of the monitored parameters. Such observation is important for the experimental community, not only in the case of a thermocouple, but also when employing other embedded elements, such as a pressure gauge, as the validation of many state-of-art models on heated concrete are based on the pressure measurements.

The 3D information from tomography also gives insight to the influence that a crack, which is not visible with naked eye, can have on the drying front.

It is important to emphasize that the observations presented in this study are based on small scale experiments (d=3 cm). Such kind of experiments are crucial for understanding the physical phenomena involved in fire spalling of concrete. In addition, they provide important data for validating the numerical models for predicting spalling. Therefore, the authors believe that the findings presented hereby reveal important information for the experimental community on concrete at high temperature and can be employed in the perspective of improving the experimental procedures.

Acknowledgements This study was partially financed by LabEx TEC21 (Investissements d'Avenir-grant agreement n° ANR-11-LABX-0030). The authors gratefully acknowledge Université Grenoble-Alpes and Empa Laboratories for supporting this experimental campaign.

References

1. E. Richter, in *Fire Design of Concrete Structures: What now? What next?* (2004), pp. 261–268
2. L. Boström, J. Robert, Report in SP Technical Research Institute of Sweden (2008)
3. S. Dal Pont, A. Ehrlacher, International Journal of Heat and Mass Transfer **47**(1), 135 (2004). DOI https://doi.org/10.1016/S0017-9310(03)00381-8
4. H. Carre, P. Pimienta, C. La Borderie, F. Pereira, J.C. Mindeguia, MATEC Web of Conferences **6**, 01007 (2013). DOI 10.1051/matecconf/20130601007
5. F. Pereira, K. Pistol, M. Korzen, F. Weise, P. Pimienta, H. Carré, S. Huismann, in *2nd International RILEM Workshop on Concrete Spalling due to Fire Exposure* (2011), pp. 369–377
6. F. Lo Monte, R. Felicetti, Materials and Structures **50**(4), 192 (2017). DOI 10.1617/s11527-017-1055-1
7. P. Kalifa, F.D. Menneteau, D. Quenard, Cement and Concrete Research **30**(12), 1915 (2000). DOI http://dx.doi.org/10.1016/S0008-8846(00)00384-7
8. S. Dal Pont, H. Colina, A. Dupas, A. Ehrlacher, Magazine of Concrete Research **57**(8), 455 (2005). DOI 10.1680/macr.2005.57.8.455
9. K. Hertz, L. Sørensen, Fire Safety Journal **40**(5), 466 (2005). DOI 10.1016/j.firesaf.2005.04.001
10. G. Van der Heijden, L. Pel, O. Adan, Cement and Concrete Research **42**(2), 265 (2012). DOI https://doi.org/10.1016/j.cemconres.2011.09.014
11. R. Felicetti, F. Lo Monte, MATEC Web of Conferences **6**, 03001 (2013). DOI 10.1051/matecconf/20130603001
12. T. Tanibe, M. Ozawa, R. Kamata, K. Rokugo, Journal of Structural Fire Engineering **5**(3), 239 (2014). DOI 10.1260/2040-2317.5.3.239
13. N. Toropovs, F. Lo Monte, M. Wyrzykowski, B. Weber, G. Sahmenko, P. Vontobel, R. Felicetti, P. Lura, Cement and Concrete Research **68**, 166 (2015). DOI http://dx.doi.org/10.1016/j.cemconres.2014.11.003
14. F. Lo Monte, F. Lombardi, R. Felicetti, M. Lualdi, Construction and Building Materials **151**, 881 (2017). DOI https://doi.org/10.1016/j.conbuildmat.2017.06.114. URL `http://www.sciencedirect.com/science/article/pii/S0950061817312503`
15. R. Felicetti, F. Lo Monte, P. Pimienta, Cement and Concrete Research **94**, 13 (2017). DOI https://doi.org/10.1016/j.cemconres.2017.01.002
16. J.C. Mindeguia, P. Pimienta, A. Noumowé, M. Kanema, Cement and Concrete Research **40**(3), 477 (2010). DOI http://dx.doi.org/10.1016/j.cemconres.2009.10.011
17. R. Mugume, T. Horiguchi, MATEC Web of Conferences **6**, 03002 (2013). DOI 10.1051/matecconf/20130603002
18. D. Dauti, A. Tengattini, S. Dal Pont, N. Toropovs, M. Briffaut, B. Weber, Cement and Concrete Research **111**, 41 (2018). DOI https://doi.org/10.1016/j.cemconres.2018.06.010

19. G. Van der Heijden, H. Huinink, L. Pel, K. Kopinga, Journal of Magnetic Resonance **208**(2), 235 (2011). DOI https://doi.org/10.1016/j.jmr.2010.11.010
20. S. Dal Pont, Lien entre la perméabilité et l'endommagement dans les bétons à haute température. Ph.D. thesis, ENPC (2004)
21. R. Jansson, Material properties related to fire spalling of concrete. Licentiate thesis, Division of Building Materials (2008)
22. R. Jansson, Fire spalling of concrete : Theoretical and experimental studies. Ph.D. thesis, KTH, Concrete Structures (2013)
23. R.B. Mugume, T. Horiguchi, in *2nd International RILEM Workshop on Concrete Spalling due to Fire Exposure* (2011), pp. 87–94
24. D. Dauti, S. Dal Pont, B. Weber, M. Briffaut, N. Toropovs, M. Wyrzykowski, G. Sciumé, International Journal for Numerical and Analytical Methods in Geomechanics **42**(13), 1516 (2018)